Preprints.org

Article

Not peer-reviewed version

Shoreline Analysis of Sandbar Topography in the Nakdong River Estuary using SPOT Series Satellite Imagery

Sang-Hee Lee , Chang-Uk Hyun , Sung-Bo Kim *

Posted Date: 12 February 2024

doi: 10.20944/preprints202402.0616.v1

Keywords: SPOT; satellite imagery; digital shoreline analysis system (DSAS); Nakdong River Estuary; sandbar; shoreline erosion

Preprints.org is a free multidiscipline platform providing preprint service that is dedicated to making early versions of research outputs permanently available and citable. Preprints posted at Preprints.org appear in Web of Science, Crossref, Google Scholar, Scilit, Europe PMC.

Copyright: This is an open access article distributed under the Creative Commons Attribution License which permits unrestricted use, distribution, and reproduction in any medium, provided the original work is properly cited.

Preprints.org (www.preprints.org) | NOT PEER-REVIEWED | Posted: 12 February 2024 doi:10.20944/preprints202402.0616.v1

Disclaimer/Publisher's Note: The statements, opinions, and data contained in all publications are solely those of the individual author(s) and contributor(s) and not of MDPI and/or the editor(s). MDPI and/or the editor(s) disclaim responsibility for any injury to people or property resulting from any ideas, methods, instructions, or products referred to in the content.

Article

Shoreline Analysis of Sandbar Topography in the Nakdong River Estuary using SPOT Series Satellite Imagery

Sang-Hee Lee [1], Chang-Uk Hyun [1] and Sung-Bo Kim [2,*]

[1] Department of Future Energy Engineering, Dong-A University, Busan 49315, South Korea; e-mail@e-mail.com; lsh3314@naver.com (S-H.L.); cuhyun@dau.ac.kr (C-U.H.)
[2] Department of Drone and Spatial Information Engineering, Young-San University, Yangsan 50510, South Korea; e-mail@e-mail.com (S-B.K.)
* Correspondence: tamsabo@ysu.ac.kr; Tel.: +82-55-380-9504

Abstract: Here, satellite images from 2006 to 2022 were collected to assess changes in the sandbar topography of the Nakdong River Estuary region, southeast of South Korea. The employed method of satellite image acquisition involves capturing images at the same time each year to facilitate a comparison of topographical changes over time. The shorelines of the islands in the study area, including Jinwoo Island, Shinja Island, and Doyo Sandbar, were analyzed. Shoreline analysis was performed using the digital shoreline analysis system (DSAS) package in ArcGIS. The results indicate that Jinwoo Island is expanding at 6.46 m/year in the direction of Nulcha Island. The western side of Shinja Island is expanding at 4.76 m/year, whereas the eastern side is retreating at a rate of 24.41 m/year. In the case of the Doyo Sandbar, the southern shoreline is retreating at a rate of 14.69 m/year; however, the speed is gradually decreasing. Marked topographical changes are evident in the Nakdong River Estuary, and the interlinked barrier islands undergo deposition and erosion, leading to alterations in the shoreline. These findings serve as foundational data for predicting and addressing environmental and social issues arising in the Nakdong River Estuary region due to climate change.

Keywords: SPOT; satellite imagery; digital shoreline analysis system (DSAS); Nakdong River Estuary; sandbar; shoreline erosion

1. Introduction

The Shore sandbars develop around a river estuary where the river meets the sea; islands formed in this manner are referred to as barrier islands. Barrier islands are depositional landforms influenced by the tidal and riverine influx of sediments. They aid in obstructing incoming waves from the sea, thereby decreasing the risk of storm surges and tidal flooding caused by typhoons. In the Nakdong River Estuary, islands such as Jinwoo Island, Shinja Island, and Doyo Sandbar provide habitats for diverse flora and fauna at the interface of terrestrial and marine environments [1].

Shoreline analysis plays a vital role in the complex study of shore topography and environments, involving various academic disciplines such as geography, environmental science, geomorphology, geology, and oceanography. Erosion, deposition, and shoreline changes along the South Korean coast occur in diverse forms owing to natural and anthropogenic factors [2]. Natural factors include sea-level rise, increased intensity and frequency of typhoons, droughts caused by global warming, heavy rainfall, and other natural disasters. Anthropogenic factors encompass human-made interventions, such as shore seawalls, port construction, and estuary dikes. Hence, maintaining continuous monitoring and implementing appropriate actions in this context is imperative [3].

Numerous studies have been conducted on the factors influencing shore changes. In Vietnam, studies have examined shore changes related to weather conditions and human activities [4]. Global

© 2024 by the author(s). Distributed under a Creative Commons CC BY license.

Preprints.org (www.preprints.org) | NOT PEER-REVIEWED | Posted: 12 February 2024 doi:10.20944/preprints202402.0616.v1

studies have been conducted on long-term changes in shorelines due to waves and storm surges [5], along with investigations into the causal factors driving shoreline changes in Southeast Asian Islands from 1990 to 2015 [6]. Gonçalves et al. [7] proposed a fuzzy model integrating shoreline changes, normalized difference vegetation index (NDVI), and settlement impacts to classify human impacts on shore areas. The model aims to enhance numerical-linguistic fuzzy classification through the graphical visualisation capabilities of geographic information systems (GIS). Hossen and Sultana [8] used geographic, spatial, and statistical methods to estimate the spatial and temporal shoreline changes on Saint Martin Island in North America from 1974 to 2021, predicting the anticipated changes between 2032 and 2042.

Over the past few decades, monitoring of shore areas worldwide has primarily relied on accurate but expensive field surveys of a limited number of beaches. However, satellite remote sensing has transformed shore science from a data-deficient to a data-rich field, offering advantages such as overcoming spatiotemporal limitations and facilitating cost-effective observations [9]. Maiti and Bhattacharya [10] investigated cost-effective alternative methods for satellite remote-sensing images and statistics. Therefore, currently, satellite imagery remains the most effective method for observing shoreline changes.

Shoreline changes are substantially influenced by sediment influx from rivers and the impact of sea-level changes. Therefore, future shoreline changes can be predicted by recording events such as floods and typhoons. This predictive information can be used for efficient shore management, marine safety, and sustainable utilisation, development, and preservation of shore resources for activities such as maritime tourism.

Shoreline analysis using satellite imagery has been extensively studied worldwide. Studies have been conducted in the Asian regions of South Korea [11–13], China [14], India [15], and Pakistan [16].

Research has been conducted in Central and South America, Mexico [17,18] and Chile [19]. Additionally, studies have been conducted in Europe and Africa, focusing on changes in the shoreline of the North Sinai coast of Egypt [20], and shoreline analysis based on Landsat satellite images has been performed in the Sopot region of northern Poland [21].

Arriola-Velásquez et al. [22] applied natural radionuclides to El Confital Bay, Spain, to study shore sediment transport as an alternative tool for shore-zone management. Nijamir et al. [23] investigated the mid-term shore changes in Augusta Bay, Italy, from 1972 to 2021. They utilised the normalised difference water index (NDWI) and modified NDWI (mNDWI) methods to analyse shorelines from Landsat and Sentinel-2 satellite images to evaluate future shore protection measures. Cenci et al. [24] measured past and present shoreline changes for shore risk management using satellite imagery and GIS technology information system technology.

Extensive research has been conducted in the study area, the sandbar region in the Nakdong River Estuary, South Korea. Kim [1] indicated that artificial environmental changes, such as estuary barrages, have led to sediment supply, promoting the growth of islands, such as Shinja Island and Doyo Sandbar. In the case of Jinwoo Island, research has suggested minimal changes in its area. Additionally, studies have shown predominant deposition in the tidal flats between mainland China, Jinwoo Island, and Shinja Island. However, research [25] has indicated that the tidal flat east of the Nakdong River Estuary on Eulsuk Island is experiencing erosion.

In this study, we utilised SPOT series satellite imagery to analyse shore changes in the sandbar region of the Nakdong River Estuary, focusing on the erosion and deposition of barrier islands. The analysis was conducted using the digital shoreline analysis system (DSAS) package in ArcGIS software. Based on a literature review, we present a comprehensive approach for remote sensing imagery and shoreline extraction. We explored the combined use of SPOT satellite imagery and the DSAS program, comprehensively reviewed shoreline extraction methods, and examined various shoreline characteristics and the methods used for their extraction. We investigated the evolution of key methods for automatic shoreline extraction, shoreline edge detection, and combinations of data from different time periods. Additionally, this paper compiles various types of shoreline extraction methods and discusses the current challenges and issues in the science of shoreline detection and extraction. In this study, we discuss the diverse applicability of data and shoreline identification

Preprints.org (www.preprints.org) | NOT PEER-REVIEWED | Posted: 12 February 2024 doi:10.20944/preprints202402.0616.v1

categories for shoreline analysis using satellite imagery spanning approximately 20 years, from 2002 to 2022. The study was conducted using the following procedure:

(1) Data collection: Satellite imagery from 2002 to 2022 was collected for the study.
(2) Image fusion: High-resolution black-and-white images were fused with low-resolution multispectral images to generate high-resolution multispectral images.
(3) Shoreline extraction: The NDWI was employed to create a feature dataset, and the shoreline was extracted using this dataset.
(4) Shoreline change study: The extracted shoreline data served as the basis for studying shoreline changes over a 20-year period.

Through this process, a feature dataset was created using the water index to study shoreline changes.

2. Materials and Methods

2.1. Study Area

As shown in Figure 1, the study area is located within the estuary of the Nakdong River at the southeast end of the Korean Peninsula. This region serves as the confluence point where the Nakdong River meets the sea. As a considerable amount of suspended sediment transported from the upstream Nakdong River flows downstream, the water depth decreases and the flow velocity diminishes, leading to the deposition of particles and formation of sandbars of various sizes parallel to the shoreline. This topographical change has resulted in the formation of diverse islands such as Eulsuk Island, Hajung Island, Jinwoo Island, Shinja Island, and Doyo Sandbar, along with sandbars such as the Baekhap, Daema, and Maenggeummori sandbars. The Nakdong River Estuary undergoes continuous changes influenced by external factors such as rainfall, waves, and currents, as well as powerful forces such as typhoons. In addition to these natural changes, the construction of the Nakdong River Estuary barrage in 1987 artificially controlled the mixing of freshwater and seawater, allowing mixture only when the barrage was open. This artificial regulation considerably affected the sedimentary environment of the Nakdong River Estuary. Hydraulic variations cause the formation of a new equilibrium state through the movement of sediment and its interaction with the natural topography and buoyant flow. Consequently, the Nakdong River Estuary area is predicted to experience localised erosion or deposition, leading to the potential closure of navigational routes and changes in marine ecosystems. Continuous monitoring of environmental changes is essential to prepare for future environmental shifts.

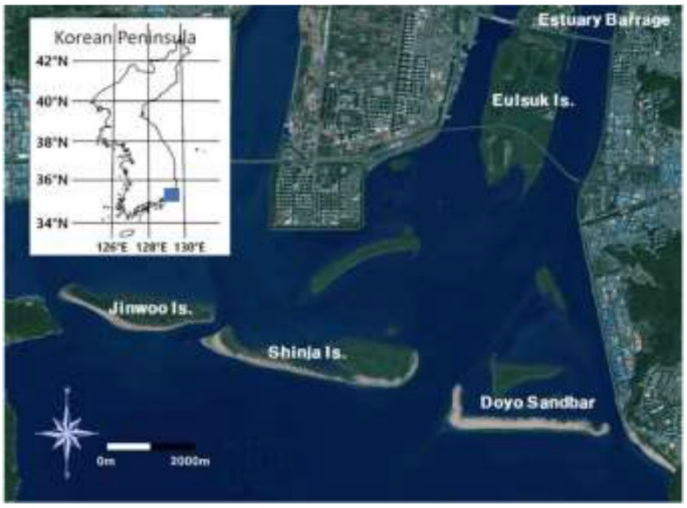

Figure 1. The location of the satellite image is the location of the blue box on the topographic map of the Korean Peninsula. Satellite image of the Nakdong River estuary in Republic of Korea (SPOT-7, October 2022).

Preprints.org (www.preprints.org) | NOT PEER-REVIEWED | Posted: 12 February 2024 doi:10.20944/preprints202402.0616.v1

2.2. Satellite Imagery Collection and Analysis

To understand shore changes in the study area, satellite imagery data captured by the French satellites SPOT-5, SPOT-6, and SPOT-7 were collected and analysed. Satellite images were acquired annually during the winter season to align with topographic changes over time for comparative analysis. Satellite images were obtained using SPOT-5 (2002–2013), SPOT-6 (2014, 2018, and 2022), and SPOT-7 (2015–2016 and 2019–2021). SPOT-5, launched in 2002, is equipped with capabilities such as high-resolution geometric (HRG) imaging, high-resolution stereoscopy (HRS), VEGETATION 2, Doppler orbitography, and radio positioning integrated with satellite next-generation radio access network (NG-RAN). SPOT-6 and SPOT-7 were launched in 2010 and 2014, respectively. SPOT-6 is equipped with two HRG sensors, one near-infrared (NIR) sensor, and three multispectral sensors. SPOT-7 is equipped with two new AstroSat optical modular instrument (NAOMI) sensors and, like SPOT-6, includes NIR sensors and three multispectral sensors. Table 1 shows the specifications of SPOT-5, SPOT-6, and SPOT-7. Additionally, Table 2 presents the satellite images collected from 2002 to 2022.

Table 1. Specifications of SPOT satellite.

Specifications	SPOT-5	SPOT-6 & 7
Launch date	2002. 05	SPOT-6: 2012.09 SPOT-7: 2014.06
Life span	5+ year	10+ year
Orbit characteristics	Rotation motive	Rotation motive
Equator cruising altitude	822 km	694 km
Orbit cycle	101.4 min	98.79 min
Same orbit cycle	26 days	26 days
Slope observation	≤45°	≤ 45°
Observation width	60 km	60 km
Spatial resolution	2.5 m (Panchromatic) 10.0 m (Multispectral)	1.5 m (Panchromatic) 6.0 m (Multispectral)

Table 2. Satellite images of the SPOT series during the research periods.

Date	Satellite Picture	Date	Satellite Picture
December 27, 2002		October 3, 2003	
November 12, 2004		November 20, 2006	

Preprints.org (www.preprints.org) | NOT PEER-REVIEWED | Posted: 12 February 2024 doi:10.20944/preprints202402.0616.v1

November 30, 2007		December 19, 2008	
December 2, 2009		November 17, 2010	
November 15, 2011		January 19, 2013	
November 4, 2014		November 30, 2015	
October 14, 2016		July 19, 2018	
October 11, 2019		October 7, 2020	
October 27, 2021		October 18, 2022	

2.3. Preprocessing Steps for Shoreline Analysis

In the Nakdong River Estuary, noticeable terrain changes occur, and the barrier islands are organically connected, leading to sedimentation, erosion, and changes in the shoreline. To understand the topographical changes, especially the shoreline changes, of the barrier islands in the Nakdong River Estuary, we acquired images from the SPOT series. Information about the SPOT series images acquired for the analysis is provided in Table 3.

Preprints.org (www.preprints.org) | NOT PEER-REVIEWED | Posted: 12 February 2024 doi:10.20944/preprints202402.0616.v1

Table 3. Information on the SPOT satellite images used in the analysis.

Date	Sensor	Spatial Resolution (m)	Digitisation (bit)
2002.12.	SPOT-5	2.5	8
2003.10.	SPOT-5	2.5	8
2004.11.	SPOT-5	2.5	8
2006.11.	SPOT-5	2.5	8
2007.11.	SPOT-5	2.5	8
2008.12.	SPOT-5	2.5	8
2009.12.	SPOT-5	2.5	8
2010.11.	SPOT-5	2.5	8
2011.11.	SPOT-5	2.5	8
2013.01.	SPOT-5	2.5	8
2014.11.	SPOT-6	1.5	16
2015.11.	SPOT-7	1.5	16
2016.10.	SPOT-7	1.5	16
2018.07.	SPOT-6	1.5	16
2019.10.	SPOT-7	1.5	16
2020.10.	SPOT-7	1.5	16
2021.10.	SPOT-7	1.5	16
2022.10.	SPOT-6	1.5	16

To analyse terrain changes in the barrier islands using satellite imagery, we first conducted satellite image preprocessing, including image fusion and geometric correction. For shoreline extraction, we used the NDWI method. Preprocessing is essential for satellite image analysis, as shown in Figure 2. The SPOT-5 images provided until 2013 were red, green, and blue (RGB) images (2.5 m) that required no specific preprocessing. SPOT-6 and SPOT-7 provided high-resolution black-and-white (1.5 m) and low-resolution multispectral (6.0 m) images, respectively. We applied image-fusion techniques to create high-resolution multispectral images for analysis. An example of the image fusion results is shown in Figure 3. The general formulation for image fusion techniques can be defined using the following equation:

$$\widehat{MS}_n = \widetilde{MS}_n + g_n(P - I_L), n = 1, \dots, N \quad (1)$$

where $\widehat{MS}_n$ represents the n^{th} band of the fused multispectral image, $\widetilde{MS}_n$ represents the n^{th} band of the multispectral image transformed to the same pixel count as the high-resolution black-and-white image P, g_n is the fusion coefficient, I_L is the virtual low-resolution image, and N denotes the number of bands in the image [26].

Preprints.org (www.preprints.org) | NOT PEER-REVIEWED | Posted: 12 February 2024 doi:10.20944/preprints202402.0616.v1

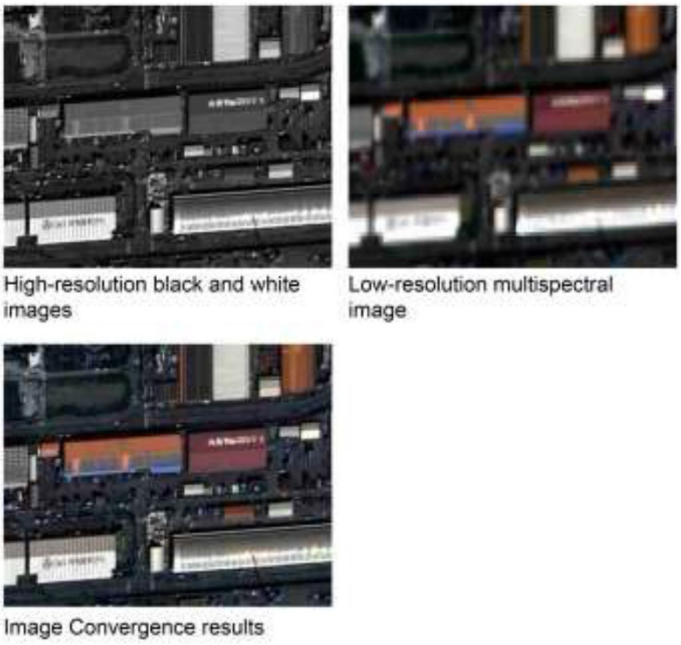

Figure 2. Image convergence results (examples near the study area).

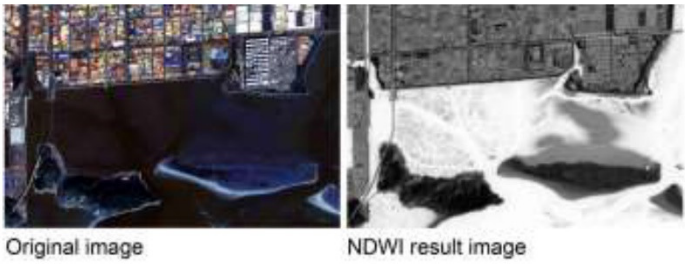

Figure 3. NDWI Result Image (examples near the study area).

For image fusion, we applied the Gram–Schmidt adaptive (GSA) technique, which is a component substitution (CS)-based fusion method. CS-based fusion methods effectively capture the spatial characteristics of high-resolution black-and-white images. The GSA fusion technique involves multiple regression analysis of high-resolution black-and-white and multispectral images to calculate I_L in Equation (1). Furthermore, the fusion coefficients g_n in the GSA technique are calculated directly using the ratios between pixels to determine the regional fusion coefficients, which are determined based on the covariance and variance relationship between multispectral images and I_L. The g_n in the GSA technique can be defined as shown in Equation (2) [26].

$$g_n = \frac{cov(I_L, MS_n)}{var(I_L)} \quad (2)$$

where var represents the variance of the image and cov denotes the covariance between the images.

For general satellite images, excluding high-resolution World View, additional corrections are required to minimise distortion for the analysis of time-series images of the same area, owing to constraints such as sensor resolution, satellite attitude, and angles during image acquisition. Manual geometric correction was performed on each image, and the images from 2019 to 2022 were transformed using the 2018 image as a reference. Ground control points in the images were selected based on artificial objects that did not change with the weather or season, and the root mean square error was set within 1 m. The RGB and NIR band information of SPOT-6 and 7 satellite images were utilised to extract the shoreline using the NDWI. The NDWI, calculated based on the relationship between the NIR and green bands, effectively extracted the water bodies. The calculated results of

Preprints.org (www.preprints.org) | NOT PEER-REVIEWED | Posted: 12 February 2024 doi:10.20944/preprints202402.0616.v1

the NDWI ranged from 0 to 1, with values closer to 1 indicating a higher probability of water bodies. Figure 3 shows an example of the calculated NDWI results.

Finally, to extract the shoreline using satellite imagery, a binary image was generated based on the NDWI results. A binary image is automatically created using Otsu's method to calculate the threshold value. For shoreline analysis, the binary image, initially in the raster format, was converted to the vector format for utilisation in the GIS software. Figure 4 displays the results of automatic binary image generation using the optimal thresholding by maximising the between-class variance (Otsu's) method from the NDWI image, along with the corresponding vector conversion. The Otsu's method is widely used in various image-processing applications, including image thresholding, segmentation, and object recognition. This is a simple and effective approach to determine the optimal threshold for image segmentation, including tasks such as object detection.

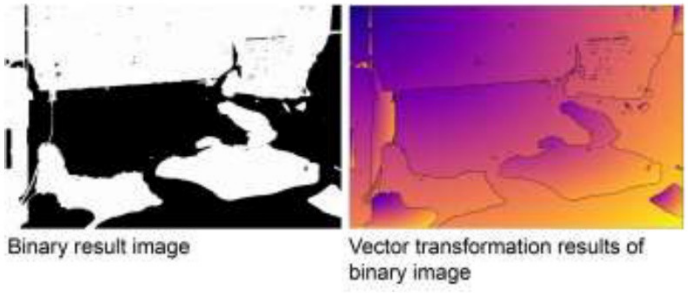

Figure 4. Binary image and vector transformation results using Otsu Techniques.

2.4. Shoreline Change Analysis

To analyse the shoreline changes, we utilised the DSAS package in ArcGIS, a representative GIS software package. The DSAS uses a reference line to calculate the four statistical elements for shoreline data and changes. The four elements include the Shoreline Change Envelope (SCE), Net Shoreline Movement (NSM), End Point Rate (EPR), and Linear Regression Rate (LRR). NSM, EPR, and LRR can have both negative and positive values depending on the nature of the changes. In this study, negative values represent shoreline retreat (erosion) towards the inside of the island, whereas positive values indicate shoreline advancement (accretion) towards the outside.

In EPR, the statistical processing of distance changes at intersections where the current shoreline and measurement line meet, performed using the reference and measurement lines, requires careful selection because it considerably influences the analysis results. To represent the current state of shoreline changes effectively, we set four to five reference lines as parallel as possible to the current shoreline for each island. The measurement lines were placed perpendicular to the reference lines at approximately 100-m intervals. The measurement lines were numbered counterclockwise from the west of each island. Figure 5 shows an example of the shoreline line-analysis process.

Preprints.org (www.preprints.org) | NOT PEER-REVIEWED | Posted: 12 February 2024 doi:10.20944/preprints202402.0616.v1

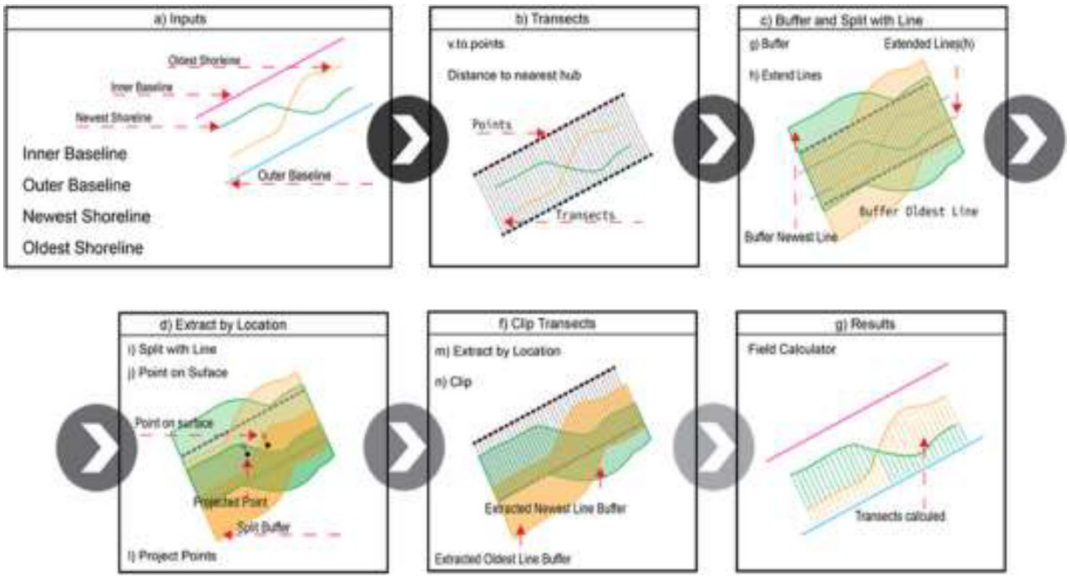

Figure 5. Example of Shoreline Analysis Process [27].

3. Analysis Results of Shoreline Changes in Barrier Islands

3.1. Analysis Results for Jinwoo Island

Figure 5 depicts the results of the shoreline analysis using the DSAS package in the ArcGIS software, allowing for the examination of shorelines and reference lines for each year. Figure 6 presents the statistical values obtained through shoreline analysis, as shown in Table 4, and Figures 7 and 8 graphically illustrate the changes in these statistical measures. The results of the shoreline analysis revealed that multiple shorelines on Jinwoo Island have expanded, especially in the western area, where the SCE, NSM, EPR, and LRR revealed consistent shoreline expansion. In contrast, the southeastern area exhibits the opposite trend, indicating a repetitive pattern of shoreline advancement and retreat. Compared with the other fenced islands, Jinwoo Island underwent relatively minor changes, with the western shoreline expanding faster than the eastern shoreline. The channels of both Nulcha Island and Shinja Island show narrow widths. In particular, the shoreline in the western direction from Jinwoo Island towards Nulcha Island is expanding at a rate of 6.46 m/year.

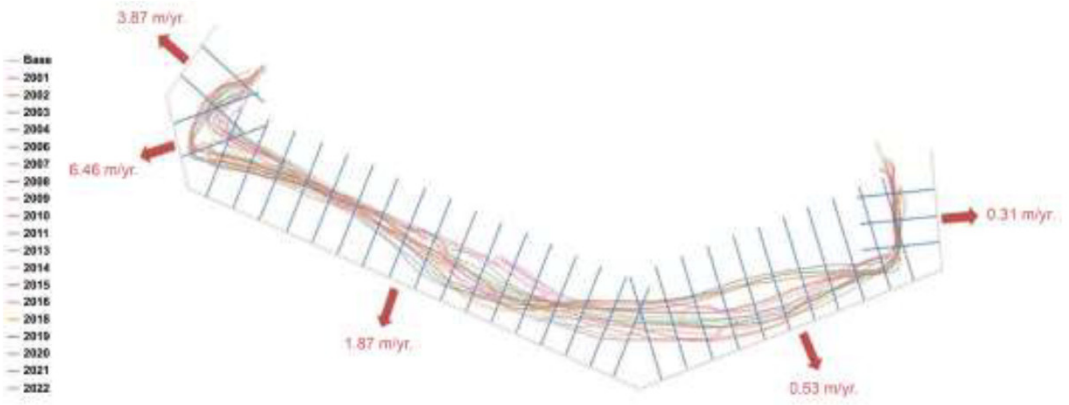

Figure 6. Jinwoo island shoreline and baseline.

Table 4. Jinwoo island shoreline change analysis results.

Baseline	Transect	SCE	NSM	EPR	LRR
BS01	JL01	72.51	42.53	2.03	2.78
	JL02	143.97	68.21	3.25	4.95

Preprints.org (www.preprints.org) | NOT PEER-REVIEWED | Posted: 12 February 2024 doi:10.20944/preprints202402.0616.v1

BS02	JL03	173.78	173.81	8.28	7.81
	JL04	209.41	158.78	7.56	5.11
BS03	JL05	131.41	88.86	4.23	2.95
	JL06	70.72	35.15	1.67	0.81
	JL07	64.58	20.82	0.99	0.03
	JL08	76.20	42.45	2.02	0.80
	JL09	56.48	32.28	1.54	0.95
	JL10	47.70	31.71	1.51	0.91
	JL11	53.78	45.97	2.19	2.86
	JL12	66.34	51.61	2.46	3.71
	JL13	84.72	75.89	3.61	5.08
	JL14	102.79	102.80	4.90	5.56
	JL15	131.65	123.48	5.88	5.83
	JL16	135.21	104.16	4.96	3.81
	JL17	113.17	100.41	4.78	3.19
	JL18	91.14	56.39	2.69	0.51
BS04	JL19	89.33	15.89	0.76	-1.45
	JL20	97.65	12.78	0.61	-1.93
	JL21	107.16	22.45	1.07	-1.78
BS04	JL22	103.68	20.72	0.99	-1.99
	JL23	118.13	32.28	1.54	-1.81
	JL24	112.28	25.82	1.23	-2.35
	JL25	88.83	1.97	0.09	-1.81
	JL26	86.28	-20.26	-0.96	1.46
	JL27	84.45	-36.19	-1.72	-0.32
	JL28	71.49	-13.98	-0.67	0.48
	JL29	75.52	25.05	1.19	0.84
	JL30	60.25	49.57	2.36	2.95
	JL31	47.83	33.56	1.60	2.83
	JL32	69.70	36.41	1.73	5.51
BS05	JL33	21.55	14.58	0.69	0.38
	JL34	19.71	13.79	0.66	-0.11
	JL35	29.13	-8.82	-0.42	0.65

* SCE (Shoreline Change Envelope) NSM, (Net Shoreline Movement) EPR, (Endpoint Rate), and LRR (Linear Regression Rate)

Preprints.org (www.preprints.org) | NOT PEER-REVIEWED | Posted: 12 February 2024 doi:10.20944/preprints202402.0616.v1

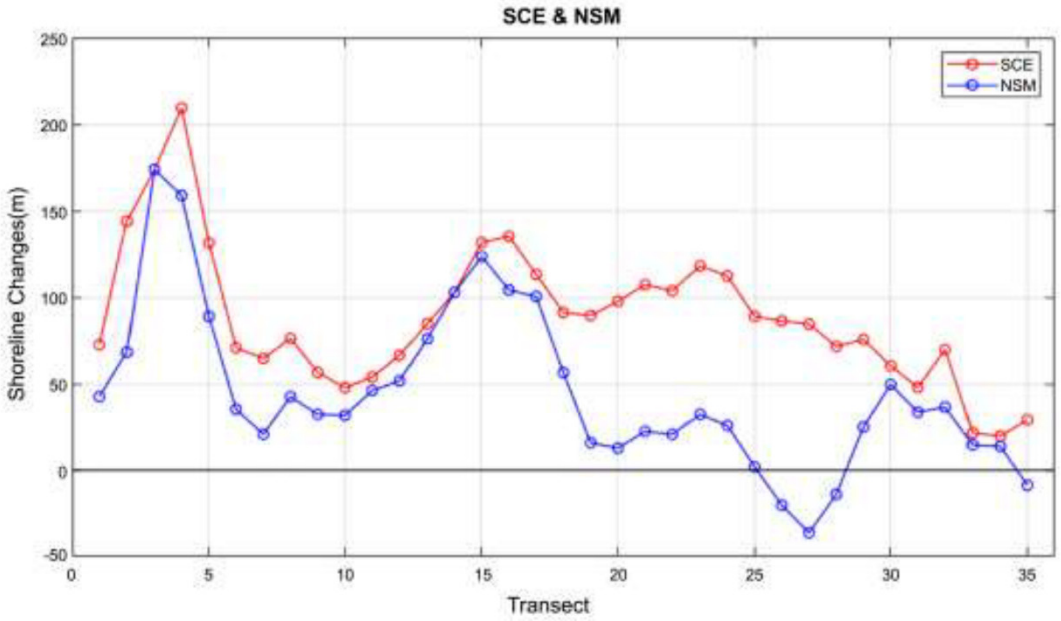

Figure 7. SCE and NSM in Jinwoo Island.

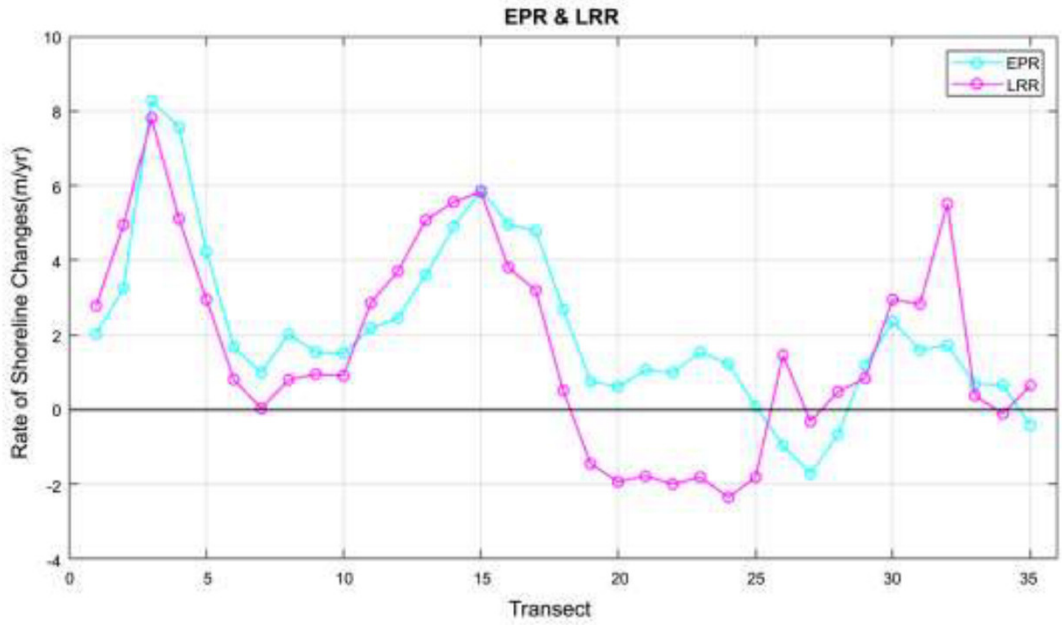

Figure 8. EPR and LRR in Jinwoo Island.

3.2. Analysis Results for Shinja Island

Shinja Island is centrally positioned among the three barrier islands in the Nakdong River Estuary. Owing to its proximity to the other islands on both sides, Shinja Island is considerably influenced by shore changes compared to the other islands. Figure 9 illustrates the annual shoreline and baseline of Shinja Island. The results obtained using the ArcGIS DASA package are presented in Table 5 and Figures 10 and 11. The western part of the island shows a shoreline expansion of 4.76 m/year, along with a reduction in the width of the channel as the eastern shoreline of Jinwoo Island expands. In contrast, the eastern part of Shinja Island exhibits a retreat at a rate of 24.41 m/year. Unlike in the western part, erosion occurred in the eastern part of Shinja Island, particularly at the tail end of the easternmost islet.

Preprints.org (www.preprints.org) | NOT PEER-REVIEWED | Posted: 12 February 2024 doi:10.20944/preprints202402.0616.v1

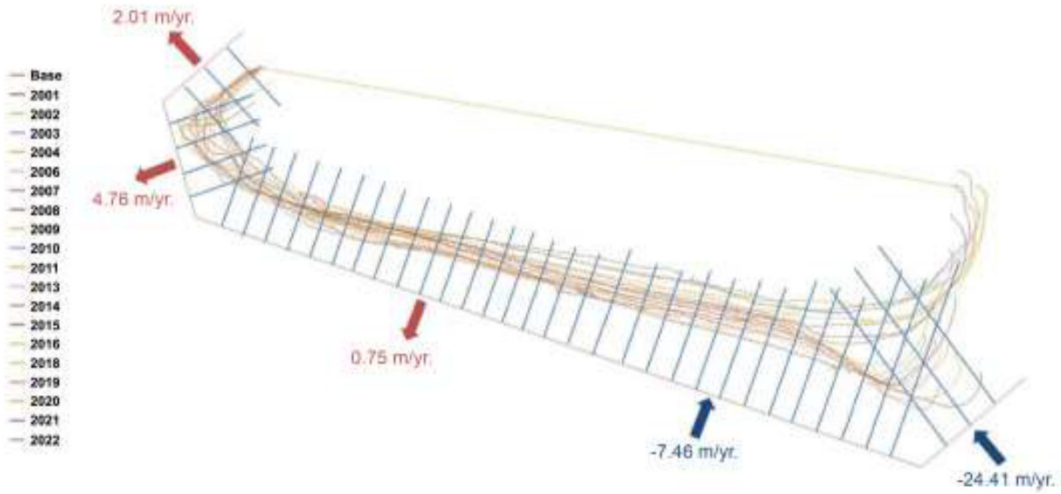

Figure 9. Shinja Island shoreline and baseline.

Table 5. Shinja Island shoreline change analysis results.

Baseline	Transect	SCE	NSM	EPR	LRR
BS01	SL01	28.88	15.67	0.75	1.04
	SL02	40.13	22.99	1.09	1.65
BS02	SL03	85.06	53.72	2.56	3.33
	SL04	167.10	167.05	7.95	6.76
	SL05	151.93	110.94	5.28	2.42
BS03	SL06	163.86	137.60	6.55	3.50
	SL07	161.61	132.08	6.29	6.11
	SL08	125.15	98.96	4.71	5.01
	SL09	131.08	109.78	5.23	4.7
	SL10	119.06	111.80	5.32	5.06
	SL11	92.02	69.10	3.29	3.32
	SL12	81.86	34.57	1.65	0.52
	SL13	91.71	41.10	1.96	0.38
	SL14	106.04	14.38	0.68	-0.94
	SL15	102.52	8.42	0.40	-0.68
	SL16	84.24	1.26	0.06	-1.22
	SL17	79.63	-2.20	-0.10	1.52
	SL18	68.16	-13.65	-0.65	0.76
	SL19	71.21	-25.31	-1.21	0.04
	SL20	74.37	-21.19	-1.01	0.60
	SL21	80.36	-27.26	-1.30	-0.78
	SL22	79.33	-51.47	-2.45	-2.78
BS04	SL23	89.32	-60.67	-2.89	-4.11
	SL24	97.31	-57.04	-2.72	-4.10
	SL25	97.72	-76.44	-3.64	-5.05
	SL26	96.96	-80.22	-3.82	-5.74
	SL27	119.48	-92.49	-4.40	-6.47
	SL28	138.57	-103.55	-4.93	-7.21
	SL29	142.70	-114.43	-5.45	-7.78
	SL30	134.51	-115.11	-5.48	-7.72

Preprints.org (www.preprints.org) | NOT PEER-REVIEWED | Posted: 12 February 2024 doi:10.20944/preprints202402.0616.v1

	SL31	128.78	-123.80	-5.90	-7.58
	SL32	126.94	-113.73	-5.42	-7.57
	SL33	119.23	-119.21	-5.68	-6.44
	SL34	104.40	-104.38	-4.97	-5.61
	SL35	125.61	-125.60	-5.98	-5.49
	SL36	160.91	-160.92	-7.66	-7.80
	SL37	225.16	-200.38	-9.54	-11.47
	SL38	166.47	-288.81	-13.75	-19.27
	SL39	212.95	-357.17	-17.01	-23.36
BS05	SL40	403.16	-411.86	-19.61	-26.02
	SL41	389.11	-385.35	-18.35	-23.86

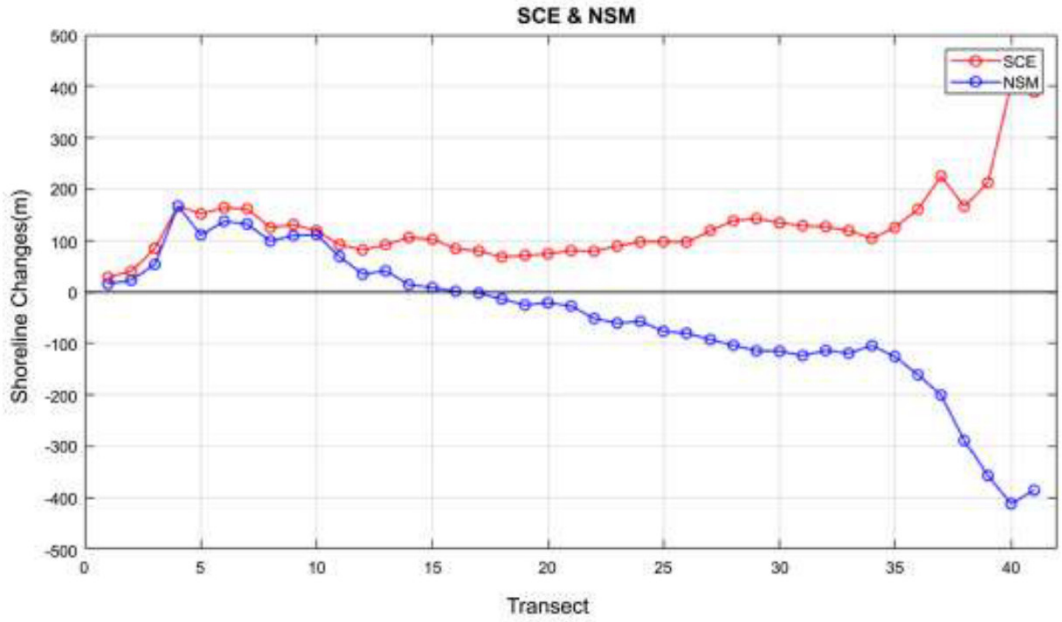

Figure 10. SCE and NSM in Shinja Island.

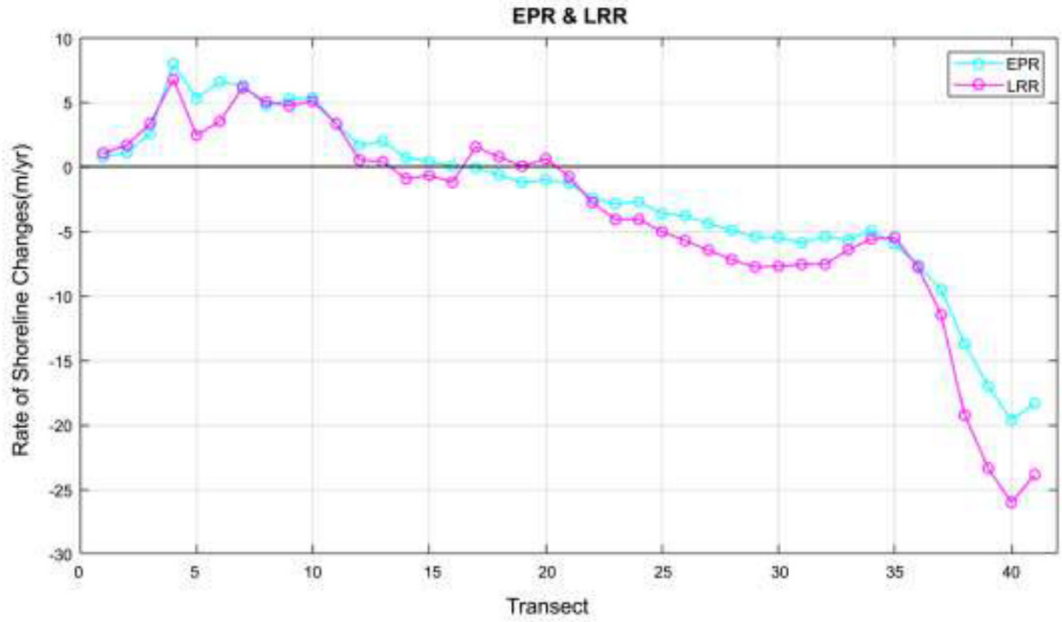

Figure 11. EPR and LRR in Shinja Island.

Preprints.org (www.preprints.org) | NOT PEER-REVIEWED | Posted: 12 February 2024 doi:10.20944/preprints202402.0616.v1

3.3. Analysis Results for Doyo Sandbar

Among the three barrier islands in the Nakdong River Estuary, the Doyo Sandbar is situated on the extreme right. The shoreline data and baseline for the Doyo Sandbar are shown in Figure 12, and the statistical results are presented in Table 6 and Figures 13 and 14. The analysis indicated shoreline retreat, with the southern shoreline retracting northward at a rate of 14.69 m/year. The EPR, LRR, SCE, and NSM exhibited similar trends. However, by comparing the shoreline locations by year, as shown in Figure 12, a gradual decrease in speed was observed. The eastern end of the Doyo Sandbar expands northward, whereas sediments are deposited on the western end due to the erosion of the West Shindo shoreline.

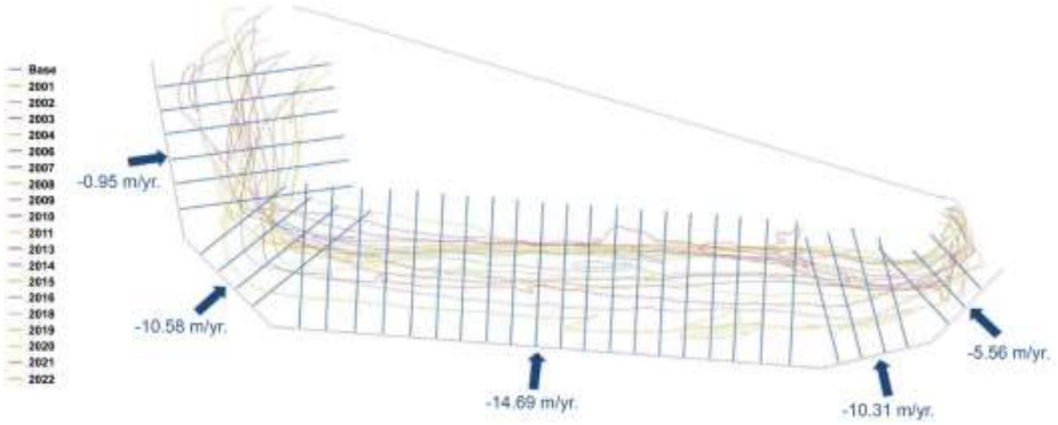

Figure 12. Doyo sandbar shoreline and baseline.

Table 6. Doyo sandbar shoreline change analysis results.

Baseline	Transect	SCE	NSM	EPR	LRR
BS01	DL01	280.78	52.63	2.51	0.79
	DL02	364.1	125.90	6.00	4.28
	DL03	240.58	-5.78	-0.28	0.14
	DL04	232.59	-83.81	-3.99	-4.87
	DL05	199.94	-117.49	-5.59	-3.47
	DL06	161.56	-124.28	-5.92	-2.54
BS02	DL07	175.99	-175.99	-8.38	-4.36
	DL08	298.11	-186.78	-8.89	-7.36
	DL09	349.37	-176.83	-8.42	-14.81
	DL10	350.68	-143.30	-6.82	-15.80
BS03	DL11	286.52	-114.85	-5.47	-11.71
	DL12	282.53	-114.11	-5.43	-12.37
	DL13	281.07	-116.09	-5.53	-12.99
	DL14	284.94	-138.00	-6.57	-13.29
	DL15	281.33	-155.85	-7.42	-14.47
	DL16	278.63	-167.16	-7.96	-14.73

Preprints.org (www.preprints.org) | NOT PEER-REVIEWED | Posted: 12 February 2024 doi:10.20944/preprints202402.0616.v1

	DL17	284.14	-180.13	-8.58	-15.95
	DL18	248.62	-188.45	-8.97	-15.71
	DL19	244.61	-204.13	-9.72	-16.31
	DL20	238.10	-196.73	-9.37	-15.27
	DL21	247.19	-203.34	-9.68	-15.96
	DL22	304.07	-220.18	-10.48	-16.95
	DL23	238.79	-214.52	-10.22	-15.79
	DL24	234.08	-183.46	-8.74	-14.82
BS03	DL25	227.26	-217.46	-10.36	-15.89
	DL26	208.95	-208.96	-9.95	-15.26
	DL27	207.69	-207.70	-9.89	-14.46
	DL28	207.59	-207.61	-9.89	-14.17
	DL29	211.07	-211.06	-10.05	-13.65
	DL30	236.52	-236.53	-11.26	-13.98
	DL31	242.82	-242.84	-11.56	-14.57
	DL32	196.47	-196.48	-9.36	-12.48
BS04	DL33	151.49	-151.50	-7.21	-7.84
	DL34	112.61	-112.59	-5.36	-6.33
	DL35	140.91	-139.81	-6.66	-7.68
BS05	DL36	143.25	-97.96	-4.66	-4.84
	DL37	151.78	-92.83	-4.42	-4.17

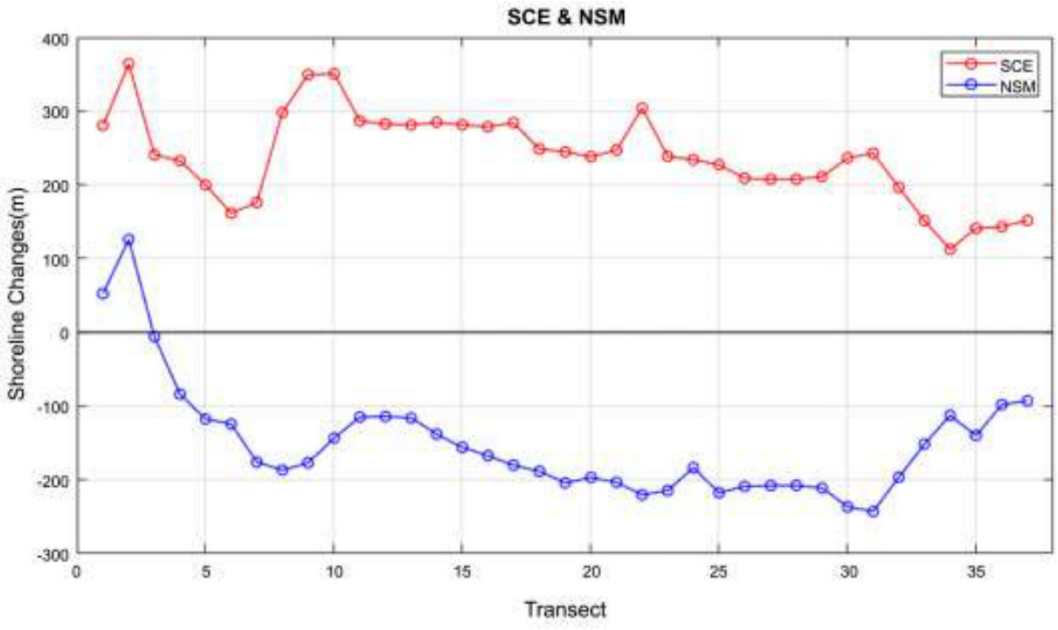

Figure 13. SCE and NSM in Doyo sandbar.

Preprints.org (www.preprints.org) | NOT PEER-REVIEWED | Posted: 12 February 2024 doi:10.20944/preprints202402.0616.v1

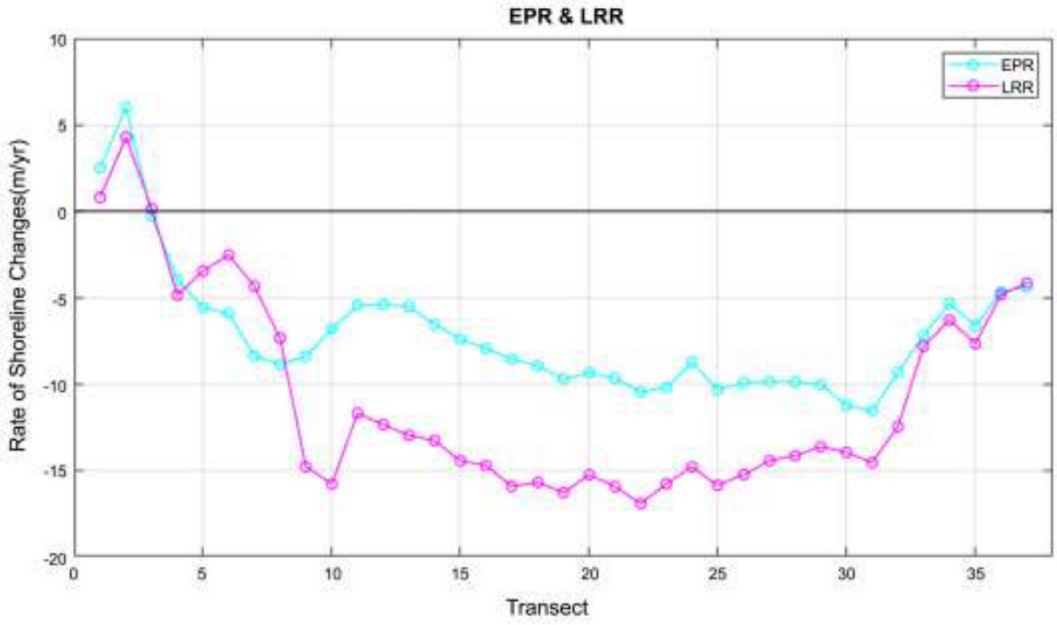

Figure 14. EPR and LRR in Doyo sandbar.

4. Discussion

This study provides a systematic analysis of coastal shoreline changes in the Nakdong River Estuary region, offering crucial foundational data applicable across various academic disciplines such as geography, geology, and environmental science. The coastal changes in this region play a pivotal role as fundamental information for understanding and preparing for the impacts on local communities and the environment.

To clarify the impact on maritime traffic, the study highlights the narrowing of the channel between Jinwoo Island and Nulcha Island, as well as the reduced width of the waterways near Doyo Sandbar and Shinja Island. These changes can influence vessel navigation, emphasising the need to develop contingency measures for maritime transportation and port operations.

Furthermore, the study reveals social issues associated with dredging. The findings indicate that the movement of the shoreline is linked to dredging and sediment handling problems, necessitating continuous monitoring and response to issues such as suspended solids and environmental degradation.

From the perspective of coastal locations and aquaculture facility placement, the study shows that the shoreline changes may affect aquaculture facilities established in the sea-front area of Jinwoo Island. This impact extends to fisheries and aquaculture, requiring ongoing monitoring and the development of appropriate measures.

The statistical analysis of shoreline changes on barrier islands underscores the importance of continuous monitoring and accurate data collection using the statistical methods proposed in the study. Statistical analysis of these changes is essential for obtaining reliable results.

The study also addresses the limitations and accuracy issues associated with remote sensing. While acknowledging the advantages of studying shoreline change rates through remote sensing, the study emphasises the need to improve the accuracy of coastal location data. Therefore, more precise data collection methods are required to enhance the accuracy of the analysis results.

The temporal variability of shoreline changes is examined in the study, with the results showing stability in most sections, except for some segments. This implies the importance of considering terrain variability and highlights the necessity for long-term monitoring.

In conclusion, the study emphasises the importance of considering accuracy and error management in interpreting results. It suggests that reliable outcomes can be obtained by considering the inaccuracies and errors associated with the remote-sensing data. The findings of this study can

Preprints.org (www.preprints.org) | NOT PEER-REVIEWED | Posted: 12 February 2024 doi:10.20944/preprints202402.0616.v1

contribute to the formulation of effective management policies and responses to potential environmental and social issues in the Nakdong River Estuary area.

5. Conclusion

In this study, we extracted and analysed the shorelines of the barrier islands (Jinwoo Island, Shinja Island, and Doyo Sandbar) in the Nakdong River Estuary using satellite imagery. Jinwoo Island exhibited minimal changes compared with the other islands, expanding in the direction of Nulcha Island to the west. Shinja Island is expanding near the western part of the island, but is rapidly eroded in the eastern part. In the Doyo Sandbar, the southern shoreline is eroding, the eastern part is expanding northward, and the western part is undergoing deposition due to the erosion of the Shinja Island shoreline to the west.

The main conclusions of this study are as follows:

(1) Jinwoo Island exhibits minimal shoreline changes compared to the other barrier islands, with the western part expanding faster than the eastern part, leading to a narrowing of the channel due to deposition. In particular, the western part of the island is expanding at a rate of 6.46 m/year.

(2) Shinja Island is experiencing shore expansion at a rate of 4.76 m/year in the western part, with a decrease in the channel width due to deposition. In contrast, the eastern part of the island is eroding at a rate of 24.41 m/year, leading to retreat.

(3) The Doyo Sandbar is experiencing a shore retreat due to erosion, with the southern shoreline retreating northward at a rate of 14.69 m/year. However, a comparison of the shoreline positions showed that the erosion rate is gradually decreasing. The eastern end of the sandbar is moving northward, whereas the western part is undergoing deposition.

As indicated by the analysis results, substantial topographical changes were evident in the Nakdong River Estuary, where barrier islands are dynamically interconnected and experience deposition and erosion, leading to shoreline changes. These shore transformations serve as foundational data for predicting and addressing social issues arising in the Nakdong River Estuary region.

This study revealed that the triangular area of the Nakdong River Estuary in the southeastern region of South Korea was influenced by complex factors, such as the discharge of freshwater due to estuarine barrage operations and the intrusion of external sea waves. Consequently, erosion-deposition cycles, primarily driven by seasonal factors, were observed during most periods. However, the long-term changes revealed distinct topographical variations. The study area is considered to have high social and environmental interest, warranting continuous and periodic field investigations. A comprehensive consideration of both conservation and development in estuarine areas is essential, as these regions are expected to be sites for large-scale maritime projects in the future. Direct bathymetric surveys are crucial for this purpose, especially for analysing the impact of meteorological factors, such as estuarine barrage discharge, on the submarine topography of the estuarine region. The integration of numerical and hydraulic modelling experiments with bathymetric survey data is necessary for long-term research. In addition, employing long-term satellite image collection is crucial for shoreline analysis.

Author Contributions: Conceptualisation, S.-B.K.; methodology, C.-U.H.; software, S.-B.K.; validation, S.-H.L.; formal analysis, C.-U.H.; investigation, S.-B.K.; resources, S.-B.K.; data curation, C.-U.H.; writing—original draft preparation, S.-H.L.; writing—review and editing, S.-H.L.; visualisation, S.- H.L.; supervision, S.-H.L.; project administration, C.-U.H.; and funding acquisition, S.-B.K. All authors have read and agreed to the published version of the manuscript.

Funding: This research was funded by the Basic Science Research Program through the National Research Foundation of Korea (NRF) supported by the Ministry of Education, grant number NRF-2022R1I1A3066000.

Institutional Review Board Statement: Not applicable.

Informed Consent Statement: Not applicable.

Data Availability Statement: Data sharing does not apply to this article.

Preprints.org (www.preprints.org) | NOT PEER-REVIEWED | Posted: 12 February 2024 doi:10.20944/preprints202402.0616.v1

Acknowledgments: None.

Conflicts of Interest: The authors declare no conflicts of interest. The sponsors had no role in the design, execution, interpretation, or writing of the study.

References

1. Kim, S.H. The morphological changes of deltaic barrier islands in the Nakdong River Estuary after the construction of river barrage. *J. Korean Geogr. Soc.* **2005,** *40*, 416–427.
2. Kim, B.J.; Kim, K.Y.; Ryu, J.H. Unmanned aerial vehicle remotely sensed datasets, a reference dataset for shore topography change and shoreline analysis. *Geo Data* **2019,** *1*, 38–45.
3. Mentaschi, L.; Vousdoukas, M.I.; Pekel, J.F.; Voukouvalas, E.; Feyen, L. Global long-term observations of shore erosion and accretion. *Sci. Rep.* **2018,** *8*, 12876.
4. Thoai, D.T.; Dang, A.N.; Oanh, N.T.K. Analysis of coastline change in relation to meteorological conditions and human activities in Ca mau Cape, VietNam. *Ocean Coast. Manag.* **2019,** *171*, 56–65.
5. Ghanavati, M.; Young, I.; Kirezci, E.; Ranasinghe, R.; Duong, T.M.; Luijendijk, A.P. An assessment of Whether long-term global changes in waves and storm surges have impacted global coastlines. *Sci. Rep.* **2023,** *13*, 11549.
6. Zhang, Y.; Li, D.; Fan, C.; Xu, H.; Hou, X. Southeast Asia island coastline changes and driving forces from 1990 to 2015. *Ocean Coast. Manag.* **2021,** *215*, 105967.
7. Gonçalves, R.M.; Saleem, A.; Queiroz, H.A.; Awange, J.L. A fuzzy model integrating shoreline changes, NDVI and settlement influences for shore zone human impact classification. *Appl. Geogr.* **2019,** *113*, 102093.
8. Hossen, M.F.; Sultana, N. Shoreline Change Detection using DSAS technique: Case of Saint Martin Island, Bangladesh. *Remote Sens Appl.: Soc. Environ.* **2023,** *30*, 100943.
9. Vitousek, S.; Buscombe, D.; Vos, K.; Barnard, P.L.; Ritchie, A.C.; Warrick, J.A. The future of shore monitoring through satellite remote sensing. *Cambridge Prisms: Coastal Futures* **2023,** *1*, e10.
10. Maiti, S.; Bhattacharya, A.K. Shoreline change analysis and its application to prediction: A remote sensing and statistics based approach. *Mar. Geol.* **2009,** *257*, 11–23.
11. Ahn, S.H.; Kim, K.H.; Lee, H.N. Analysis of coastline changes in Yeongdong Region using aerial photos and CORONA satellite images. *J. Korean Soc. Surv. Geod. Photogramm. Cartogr.* **2022,** *40*, 187–193.
12. Kim, M.K.; Yoon, J.S. Characteristic analysis of Songdo Beach, Busan, shoreline changes. *J. Ocean Eng. Technol.* **2010,** *24*, 53–59.
13. Yun, K.H.; Lee, C.K.; Kim, G.S. Estimates on the long-term landform changes near Sinduri Beaches. *Korean J. Remote Sens.* **2022,** *38* (6), 1315–1328.
14. Wei, X.; Zheng, W.; Xi, C.; Shang, S. Shoreline extraction in SAR image based on advanced geometric active contour model. *Remote Sens.* **2021,** *13*, 642.
15. Bamdadinejad, M.; Ketabdari, M.J.; Chavooshi, S.M.H. Shoreline extraction using image processing of satellite imageries. *J. Indian Soc. Remote Sens.* **2021,** *49*, 2365–2375.
16. Siyal, A.A.; Solangi, G.S.; Siyal, P.; Babar, M.M.; Ansari, K. Shoreline change assessment of Indus delta using GIS-DSAS and satellite data. *Reg. Stud. Mar. Sci.* **2022,** *53*, 102405.
17. Franco-Ochoa, C.; Zambrano-Medina, Y.; Plata-Rocha, W.; Monjardín-Armenta, S.; Rodríguez-Cueto, Y.; Escudero, M.; Mendoza, E. Long-term analysis of wave climate and shoreline change along the Gulf of California. *Appl. Sci.* **2020,** *10*, 8719.
18. Franklin, G.L.; Medellín, G.; Appendini, C.M.; Gómez, J.A.; Torres-Freyermuth, A.; González, J.L.; Ruiz-Salcines, P. Impact of port development on the Northern Yucatan Peninsula Coastline. *Reg. Stud. Mar. Sci.* **2021,** *45*, 101835.
19. Briceño-De-Urbaneja, I.; Ugalde-Peralta, R.; Sánchez-García, E.; Pardo-Pascual, J.; Palomar-Vázquez, J.; Pérez-Martínez, W.; Vidal-Páez, P.and Parrao-Barrera, M. **2020**. Intra-Annual Shore Dynamics through Remote Sensors and Morphosedimentary Patterns, ReÑaca Beach and Concon Bay, Central Chile. In *IGARSS 2020-2020 IEEE International Geoscience and Remote Sensing Symposium*, 5769–5772.
20. Nassar, K.; Mahmod, W.E.; Fath, H.; Masria, A.; Nadaoka, K.; Negm, A. Shoreline change detection using DSAS technique: Case of North Sinai Coast, Egypt. *Mar. Georesources Geotechnol.* **2019,** *37*, 81–95.
21. Specht, M.; Specht, C.; Lewicka, O.; Makar, A.; Burdziakowski, P.; Dąbrowski, P. Study on the coastline evolution in Sopot (2008–2018) based on Landsat satellite imagery. *J. Mar. Sci. Eng.* **2020,** *8*, 464.

Preprints.org (www.preprints.org) | NOT PEER-REVIEWED | Posted: 12 February 2024 doi:10.20944/preprints202402.0616.v1

22. Arriola-Velásquez, A.C.; Tejera, A.; Alonso, I.; Cámara, F.; Cantaluppi, M.; Alonso, H.; Miquel-Armengol, N., Rubiano, J.G.; Martel, P. Natural radionuclides as tracers of shore sediment dynamics in El Confital Bay (Spain): Spatial distribution and relationships with sediment characteristics. *Catena* **2024,** *235*, 107672.
23. Nijamir, K.; Ameer, F.; Thennakoon, S.; Herath, J.; Iyoob, A.L.; Zahir, I.L.M.; Sabaratnam, S.; Jisna, M.V.F.; Madurapperuma, B. Geoinformatics application for estimating and forecasting of periodic shoreline changes in the East Coast of Ampara District, Sri Lanka. *Ocean Coast. Manag.* **2023,** *232*, 106425.
24. Cenci, L.; Disperati, L.; Persichillo, M.G.; Oliveira, E.R.; Alves, F.L.; Phillips, M. Integrating remote sensing and GIS techniques for monitoring and modeling shoreline evolution to support shore risk management. *GISci. Remote Sens.* **2018,** *55*, 355–375.
25. Woo, H.J.; Lee, J.H.; Kang, J.W.; Choi, J.W.; Jong, E.J. **2018**. Sedimentary Processes of Barrier Island System in the Nakdong River Estuary. In *2018 Korea Geoscience Union Academic Conference*, 47.
26. Park, H.; Kim, N.; Park, S.; Choi, J. Sharpening of Worldview-3 satellite images by generating optimal high-spatial-resolution images. *Appl. Sci.* **2020,** *10*, 7313.
27. Terres de Lima, L.; Fernández-Fernández, S.; Marcel de Almeida Espinoza, J.; da Guia Albuquerque, M.; Bernardes, C. End point rate tool for QGIS (EPR4Q): Validation using DSAS and AMBUR. *ISPRS Int. J. Geoinf.* **2021,** *10*, 162.

Disclaimer/Publisher's Note: The statements, opinions and data contained in all publications are solely those of the individual author(s) and contributor(s) and not of MDPI and/or the editor(s). MDPI and/or the editor(s) disclaim responsibility for any injury to people or property resulting from any ideas, methods, instructions or products referred to in the content.